

Carbon and Oxygen Abundances in the Hot Jupiter Exoplanet Host Star XO-2N and its Binary Companion*

Johanna K. Teske¹, Simon C. Schuler², Katia Cunha^{1,3}, Verne V. Smith⁴, Caitlin A.
Griffith⁵

Received _____; accepted _____

*Based on data collected at Subaru Telescope, which is operated by the National Astronomical Observatory of Japan.

¹Steward Observatory, University of Arizona, Tucson, AZ, 85721, USA; email: jteske@as.arizona.edu

²University of Tampa, 401 W. Kennedy Blvd., Tampa, FL 33606, USA

³Observatório Nacional, Rua General José Cristino, 77, 20921-400, São Cristóvão, Rio de Janeiro, RJ, Brazil

⁴National Optical Astronomy Observatory, 950 North Cherry Avenue, Tucson, AZ 85719, USA

⁵Lunar and Planetary Laboratory, University of Arizona, Tucson, AZ, 85721, USA

ABSTRACT

With the aim of connecting the compositions of stars and planets, we present the abundances of carbon and oxygen, as well as iron and nickel, for the transiting exoplanet host star XO-2N and its wide-separation binary companion XO-2S. Stellar parameters are derived from high-resolution, high-signal-to-noise spectra, and the two stars are found to be similar in their T_{eff} , $\log g$, iron ($[\text{Fe}/\text{H}]$), nickel ($[\text{Ni}/\text{H}]$) abundances. Their carbon ($[\text{C}/\text{H}]$) and oxygen ($[\text{O}/\text{H}]$) abundances also overlap within errors, although XO-2N may be slightly more C-rich and O-rich than XO-2S. The C/O ratios of both stars ($\sim 0.60 \pm 0.20$) may also be somewhat larger than solar ($\text{C}/\text{O} \sim 0.50$). The XO-2 system has a transiting hot Jupiter orbiting one binary component but not the other, allowing us to probe the potential effects planet formation might have on the host star composition. Additionally, with multiple observations of its atmosphere the transiting exoplanet XO-2b lends itself to compositional analysis, which can be compared to the natal chemical environment established by our binary star elemental abundances. This work sets the stage for determining how similar/different exoplanet and host star compositions are, and the implications for planet formation, by discussing the C/O ratio measurements in the unique environment of a visual binary system with one star hosting a transiting hot Jupiter.

Subject headings: planets and satellites: formation — planets and satellites: individual (XO-2) — stars: abundances — stars: atmospheres

1. Introduction

Although theory and observations indicate that host-star composition affects planetary evolution, the physical processes responsible are not well understood. Until recently, investigations of the chemical connection between stars and planets were limited to measurements of the host star abundances. One of the most prominent findings is that the (solar-type) host stars of large, closely orbiting (hot Jupiter) exoplanets are more metal-rich than (solar-type) stars without detected gas giant exoplanets (e.g., Gonzalez et al. 1998; Santos et al. 2004; Fischer & Valenti 2005). However, the host star metallicity trend is weaker for Neptune-sized planets (e.g., Ghezzi et al. 2010) and has been found to *not* hold for terrestrial-sized planets (Buchhave et al. 2012), whose host stars show a wide range of metallicities.

With the discovery of transiting exoplanets, planetary atmospheres themselves can be observed, and their compositions determined. Indeed, the *Hubble Space Telescope* and *Spitzer Space Telescope* have been used to detect the most abundant molecules (H_2O , CO , CH_4 , CO_2) in the atmospheres of several of the brightest transiting planets (e.g., Tinetti et al. 2007; Swain et al. 2008; D  sert et al. 2009). Measurements of both stellar and exoplanetary atmospheres combined provide valuable insight into planet formation processes. The ratio of carbon to oxygen is important to interpreting hot Jupiter exoplanet spectra because they are dominated by the main carbon- and oxygen-containing molecules and particularly sensitive to different chemistry induced by different C/O ratios. In thermochemical equilibrium, at the temperatures and pressures characteristic of gas giant atmospheres, a high C/O ratio causes differences in the partitioning of C and O among H_2O , CO , CH_4 , CO_2 compared to that expected in solar abundance atmospheres ($\text{C}/\text{O}_\odot = 0.55 \pm 0.10$; Asplund et al. 2009; Caffau et al. 2011) (Kuchner & Seager 2005; Kopparapu et al. 2012; Madhusudhan 2012). This in turn affects the composition and

thermal structure, and therefore spectral signatures, of exoplanet atmospheres. Currently a number of teams are working towards establishing the C/O ratios of transiting exoplanets (e.g., Madhusudhan 2012). Observations of the host stars are needed to interpret the exoplanet observations in the context of the elemental composition of each star-planet system.

The C/O ratio of an exoplanet can also give clues as to where in the protoplanetary disk it formed (Stevenson & Lunine 1988; Öberg et al. 2011). Observations indicate that disks are inhomogeneous in physical structure and composition (e.g., Bergin 2011), but that in particular carbon and oxygen in a planet’s atmosphere could be indicative of its starting orbital position and evolution (Öberg et al. 2011). Some studies suggest that a planet may also affect the elemental composition of the host star (e.g., Meléndez et al. 2009; Ramírez et al. 2009). It is important to be able to isolate these two potential effects – the effect of the planet on the star’s elemental abundances, and the starting (or unperturbed) abundance of the system from which one can study a planet’s origin and evolution. Studies of binary star systems, as conducted here, provide a method for decoupling these two potential effects.

Reported in this paper are the C/O¹ ratios of a transiting exoplanet host star and its binary companion. We describe the XO-2 binary system, which consists of the hot Jupiter host XO-2N, and its companion XO-2S, located ~ 4600 AU away and not known to host a Hot Jupiter-type planet (Burke et al. 2007). The hot Jupiter XO-2b has an $M \times \sin i$ of $0.62 \pm 0.02 M_J$ (Narita et al. 2011), a radius of $0.97 \pm 0.03 R_J$ (Burke et al. 2007), and orbits at ~ 0.04 AU from XO-2N. The exoplanet XO-2b is one of the best characterized bodies outside the solar system, studied extensively with HST and *Spitzer* (e.g., Machalek

¹The C/O ratio – the ratio of carbon atom to oxygen atoms – is calculated in stellar abundance analysis as $C/O = N_C/N_O = 10^{\log N(C)} / 10^{\log N(O)}$ where $\log(N_X) = \log_{10}(N_X/N_H) + 12$.

² $i = 88.7 \pm 1.3^\circ$, meaning $\sin i$ is nearly unity

et al. 2009; Crouzet et al. 2012). We perform a stellar abundance analysis of both binary components to investigate the potential chemical effects of exoplanet formation.

2. Observations and Data Reduction

Observations of XO-2N and XO-2S were conducted during two half-nights, February 10 and 11 2012 (UT), with the 8.2 m Subaru Telescope using the High Dispersion Spectrograph (HDS; Noguchi et al. 2002). Spectra of the Sun (as reflected moonlight) were taken the first night, and spectra of a telluric standard (HR 6618) were taken on both nights. A 0."6 slit width was used, providing a resolution of $R = \frac{\lambda}{\Delta\lambda} = 60,000$, with two-pixel binning in the cross-dispersion direction and no binning in the dispersion direction. Across the two detectors, wavelength coverage of the spectra is $\sim 4450 \text{ \AA}$ - 5660 \AA and $\sim 5860 \text{ \AA}$ - 7100 \AA . The signal-to-noise (S/N) ratios in the combined frames ranged from ~ 170 - 230 . The raw data were reduced using standard techniques within the IRAF³ software package.

3. Abundance Analysis and Results

Stellar parameters (T_{eff} , $\log g$, microturbulence [ξ]) and elemental abundance ratios were derived following the procedures in Schuler et al. (2011a) and Cunha et al. (1998). We used the spectra themselves to determine the parameters by forcing zero correlation between $[\text{Fe I/H}]$ and lower excitation potential (χ), and between $[\text{Fe I/H}]$ and reduced

³IRAF is distributed by the National Optical Astronomy Observatory, which is operated by the Association of Universities for Research in Astronomy, Inc., under cooperative agreement with the National Science Foundation.

equivalent width $[\log(\text{EW}/\lambda)]$, as well as ensuring that the $[\text{Fe}/\text{H}]^4$ abundances derived from Fe I and Fe II lines were equal to within two significant figures. The abundances were determined using an updated version of the local thermodynamic equilibrium (LTE) spectral analysis code MOOG (Snedden 1973), with model atmospheres interpolated from the Kurucz ATLAS9 grids⁵. All abundances were normalized to solar values on a line-by-line basis. Abundances of Fe, Ni, and C were derived directly from equivalent width (EW) measurements of spectral lines in each target (with the “abfind” driver in MOOG). The EW measurements were performed with either the one-dimensional spectrum analysis package SPECTRE (Fitzpatrick & Sneden 1987) or the ‘splot’ task in IRAF.

Specifically, Fe lines were chosen from the Schuler et al. (2011a) line list. We measured 49 Fe I lines in XO-2N and XO-2S, and 8 and 10 Fe II lines in XO-2N and XO-2S, respectively. Lower excitation potentials and transition probabilities ($\log gf$) were taken from the Vienna Atomic Line Database (VALD; Kupka et al. 1999) for Fe, C, and Ni.

Carbon abundances for XO-2N and XO-2S were derived from two C I lines at 5052 Å and 5380 Å, which have been shown to provide reliable abundances in solar-type stars (Takeda & Honda 2005). Oxygen abundances were derived from the forbidden [O I] line at $\lambda = 6300.3$ Å, which is well-described by LTE (e.g. Takeda 2003); we used the Allende Prieto et al. (2001) $\log gf$ value of [O I] line. Our analysis of the forbidden oxygen line used the spectrum synthesis method (with the “synth” driver in MOOG; see Figure 1) to account for its blending with a Ni I line and a CN line. The free parameters of the synthesis fit were the continuum normalization, wavelength shift (left/right), line broadening, and oxygen abundance; we used our measured Ni and C abundances for each star, and N scaled from

⁴We use the standard bracket notation to indicate abundances relative to solar, e.g., $[\text{X}/\text{H}] = \log(N_{\text{X}}) - \log(N_{\text{X}})_{\text{solar}}$

⁵See <http://kurucz.harvard.edu/grids.html>

solar based on the measured $[\text{Fe}/\text{H}]$ of each star (e.g., Cunha et al. 1998). The Ni I line is composed of two isotopic components; the weighted $\log gf$ values of the two components from Bensby et al. (2004) were used here. We note that the [O I] line in XO-2N (with planet) required more broadening to fit with the synthesis method, suggesting it has a larger $v \sin i$ than the planet-less XO-2S.

Uncertainties in T_{eff} and ξ were calculated by forcing 1σ correlations in the relations between $[\text{Fe I}/\text{H}]$ and χ and between $[\text{Fe I}/\text{H}]$ and reduced equivalent width $[\log(\text{EW}/\lambda)]$, respectively. The change in T_{eff} or ξ required to cause a correlation coefficient r significant at the 1σ level was adopted as the uncertainty in these parameters. The uncertainty in $\log g$ was calculated differently, through an iterative process described in detail in Baubar & King (2010) and outlined in Schuler et al. (2011a).

There are two components to the uncertainties in the derived elemental abundances – one from stellar parameter errors and one from the dispersion in the abundances derived from different elemental absorption lines. To determine the uncertainty due to the stellar parameters, the sensitivity of the abundance to each parameter was calculated for changes of ± 150 K in T_{eff} , ± 0.25 dex in $\log g$, and $\pm 0.30 \text{ km s}^{-1}$ in ξ . The final uncertainty due to each parameter is then the product of this sensitivity and the corresponding parameter uncertainty (as described above). The second uncertainty component is parameterized with the uncertainty in the mean, σ_{μ}^6 , for the abundances derived from the averaging of multiple lines. Then the total uncertainty for each abundance (σ_{tot}) is the quadratic sum of the (3) individual parameter uncertainties and σ_{μ} .

The equivalent width measurements from our analysis are shown in Table 1, along

⁶ $\sigma_{\mu} = \sigma / \sqrt{N - 1}$, where σ is the standard deviation of the derived abundances and N is the number of lines used to derive the abundance.

with the wavelength, χ , $\log gf$, EWs, and line-by-line abundances for each element for the Sun, XO-2N, and XO-2S. The final derived stellar parameters and their 1σ uncertainties, as well as the derived $[\text{Fe}/\text{H}]$, $[\text{C}/\text{H}]$, $[\text{Ni}/\text{H}]$, $[\text{O}/\text{H}]$, and C/O ratio values and their 1σ uncertainties, are shown in Table 2. The C/O ratio errors are the errors of $[\text{C}/\text{H}]$ and $[\text{O}/\text{H}]$ combined in quadrature. We find $[\text{C}/\text{H}] = +0.26 \pm 0.11$ in XO-2S versus $+0.42 \pm 0.12$ in XO-2N, and $[\text{O}/\text{H}] = +0.18 \pm 0.15$ in XO-2S versus $+0.34 \pm 0.16$ in XO-2N.

In addition to our results, Table 2 lists stellar parameters and $[\text{Fe}/\text{H}]$ of Ammler-von Eiff et al. (2009) and Torres et al. (2012), two studies comparable to this one in their analysis methods and sample. Also listed are results from the exoplanet discovery paper, Burke et al. (2007). Instead of the MOOG+Kurucz models as implemented here, Burke et al. (2007) used the Spectroscopy Made Easy (SME) code (Valenti & Piskunov 1996), which has been demonstrated to be biased by correlations between T_{eff} , $[\text{Fe}/\text{H}]$, and $\log g$ as compared to a MOOG analysis (Torres et al. 2012). Their results are shown because Ammler-von Eiff et al. (2009) and Torres et al. (2012) do not include XO-2S. Our results for XO-2S differ slightly from those of Burke et al. 2007 (based on SME analysis), but our results for XO-2N are more consistent with those of Burke et al. 2007, and the same within errors as Ammler-von Eiff et al. (2009) and Torres et al. (2012), who found similarly large T_{eff} error for XO-2N.

4. Discussion

XO-2 stands out among transiting exoplanet systems because its host star, XO-2N, is in a wide binary. XO-2S, without a large, close-in planet, can be studied to determine the composition of the unperturbed environment in which these stars and planet(s) formed. We find that XO-2S and XO-2N are similar in their physical properties (with XO-2S being slightly more massive based on T_{eff} and $\log g$), as well as $[\text{Fe}/\text{H}]$ and $[\text{Ni}/\text{H}]$. The errors in

$[C/H]$ and $[O/H]$ (both relative to solar) allow for larger differences in the stars’ respective carbon and oxygen abundances (see Table 2), though within errors they also overlap. Schuler et al. (2011b) conducted a similar analysis (though did not measure O) for another roughly-equal-mass binary with one component hosting a giant planet, 16 Cyg A and B, and found the two stars to be chemically homogeneous (aside from Li and B, attributed to different internal mixing efficiencies). Our results for the XO-2 transiting planet system also indicate that the stars are chemically alike – here we additionally determine the binary stars’ C/O ratios and find both to have $C/O \sim 0.60$.

It is currently unclear whether and how planets affect the composition of the host star (e.g., Meléndez et al. 2009; Ramírez et al. 2009; Chambers 2010; González Hernández et al. 2010; Schuler et al. 2011a & 2011b). Several studies posit that stars with smaller planets are depleted in rock-forming (refractory, e.g. Mg, Si, Ni, Al) elements relative to volatile elements (e.g., C, N, O) due to rock-forming material being “locked up” in the terrestrial planets (e.g., Meléndez et al. 2009; Ramírez et al. 2009). The Sun has been shown to be deficient (by $\sim 20\%$) in refractory elements that have $T_c \gtrsim 900$ K relative to volatile elements compared to similar stars without detected planets (e.g., Meléndez et al. 2009; Ramírez et al. 2009). However, the details of how an individual star’s atmosphere is affected by the local or global composition of the disk during its evolution are uncertain. Also, we do not know whether some or even most stars hosting detected hot Jupiters actually also have small planets that might cause such a signature. The significance of our detection in both XO-2N and XO-2S of enhanced $[Fe/H]$ and $[Ni/H]$, the only two refractory abundances measured here, will be better understood when compared to a larger number of refractory elements measured in this system and the abundance trends with T_c expected based on galactic chemical evolution.

No previous study of which we are aware has uniformly derived $[C/H]$, $[O/H]$, and C/O

values for this binary system. Several studies have examined C/O ratios in non-transiting exoplanet host stars versus stars without known exoplanets. [It should be noted that any star designated as a “non-host” has the potential to harbor a smaller (undetected) planet; indeed, it may be the case that most stars have one or more small planets (e.g., Cassan et al. 2012).] Delgado Mena et al. (2010) measured carbon (using high excitation C I lines) and oxygen (using the forbidden [OI] 6300 Å line) in 100 giant planet host stars from the HARPS planet-search sample, along with 270 non-host stars. They found averaged host-star values of $[C/H]=+0.10\pm0.16$, $[O/H]=+0.05\pm0.17$, and $C/O=0.76\pm0.20$, with corresponding “single” star (no known planets) averages of $[C/H]=-0.06\pm0.18$, $[O/H]=-0.08\pm0.17$, and $C/O=0.71\pm0.18$. Similar averages, overlapping within 1σ errors, were compiled by Bond et al. (2010) and measured by Petigura & Marcy (2011). These studies show no significant difference in $[C/H]$, $[O/H]$, or C/O between stars with/without detected (non-transiting) exoplanets.

Fortney (2012) suggested the C/O ratios of both host- and non-host stars in these studies were overestimated due to errors in the derived C/O ratios and the observed frequency of carbon dwarf stars in large samples of low-mass stars. More recently, Nissen (2013) determined C/O for 33 host stars from the Delgado Mena et al. (2010) sample that had additional ESO 2.2m FEROS spectra covering the O I triplet at 7774 Å (unavailable in our data). Accounting for non-LTE effects on the [OI] triplet, Nissen (2013) found differences in derived $[O/H]$ as compared to Delgado Mena et al. (2010), resulting in a tighter correlation between $[Fe/H]$ and the C/O ratios derived by Nissen ($C/O = 0.58+0.48[Fe/H]$ with an rms dispersion $\sigma(C/O)=0.06$). However, the averaged host-star values of Nissen, (2013) overlap those of Delgado Mena et al. (2010) and the other studies listed above ($[C/H]=+0.11\pm0.15$, $[O/H]=+0.08\pm0.10$, and $C/O=0.63\pm0.12$).

The $[C/H]$ values derived here for XO-2S ($+0.26\pm0.11$) and XO-2N ($+0.42\pm0.12$) are

both larger than the averages above, and greater than solar. These stars are also enhanced in $[\text{O}/\text{H}]$ (see Table 2) and have C/O ratios of 0.60. This is the first measurement of the C/O ratio in a transiting exoplanet host star that is metal-rich. Since XO-2N and XO-2S are physically associated, the elevated $[\text{C}/\text{H}]$ and $[\text{O}/\text{H}]$ values in *both* stars are strong evidence that their parent molecular cloud was elevated in both carbon and oxygen. As shown in Figure 2, XO-2S and XO-2N follow the broad galactic chemical evolution trends in $[\text{C}/\text{H}]$, $[\text{O}/\text{H}]$, and C/O versus $[\text{Fe}/\text{H}]$ as evidenced by the large sample of Delgado Mena et al. (2010) (and also Nissen 2013). The significance of the C/O ratio derived here is supported by the careful analysis and the fact that we measured this ratio in two separate stars within the same system.

The C/O ratio of a planet does not necessarily reflect the protoplanetary-disk-averaged C/O ratio, and depends on where formation occurs, how much of the atmosphere is accreted from gas versus solids, and how isolated the atmosphere is from the core (Öberg et al. 2011). Carbon-enhanced systems may actually have more solid mass in the inner disk than solar-composition environments, due to a wide zone of C-bearing solids close to the star and a paucity of water ice farther out in the disk (Bond et al. 2010). If planets do form more readily in C-rich environments, this might help explain why there is a giant planet around XO-2N ($[\text{C}/\text{H}] = +0.42 \pm 0.12$) and not XO-2S ($[\text{C}/\text{H}] = +0.26 \pm 0.11$). However, within uncertainties, the two stars’ carbon and oxygen abundances overlap. Furthermore, Delgado Mena et al. (2010) suggest that, based on a lack of trends between C/O ratios and planetary period, semi-major axis, and mass, any effects of an alternative mass distribution due to C-rich material is quickly erased. Thus the key to understanding why XO-2N has a planet and XO-2S does not may lie in the exoplanet composition.

5. Conclusions

We present an abundance analysis for the transiting exoplanet host star XO-2N and its wide-separation binary companion XO-2S. The two stars are found to be similar in their physical and chemical properties, and both enhanced above solar in carbon and oxygen, with $C/O \sim 0.6$. Insight into why XO-2N hosts a transiting hot Jupiter, and XO-2S does not, may be revealed by the atmospheric composition and C/O ratio of the planet, which is currently being constrained with observations recorded during the its primary/secondary eclipse (e.g., Machalek et al. 2009; Crouzet et al. 2012). While previous work suggests that refractory element distributions may differ in stars with/without planets, differences in volatile elements have not been as thoroughly explored. Our results motivate further studies of planet formation and evolution with a renewed focus on volatile element distributions (particularly C and O) in both gas giant and terrestrial planets. Additional measurements of binary host star compositions will connect exoplanets and their stars and expand upon the giant planet-metallicity trend to investigate how host star chemical composition (especially C/O) influences planet formation and composition.

The authors wish to recognize and acknowledge the very significant cultural role and reverence that the summit of Mauna Kea has always had within the indigenous Hawaiian community. We are most fortunate to have the opportunity to conduct observations from this mountain. This work would not have been possible without the efforts of the daytime and nighttime support staff at the Mauna Kea Observatory and Subaru Telescope. The work of J.T. and C.G. is supported by NASA’s Planetary Atmospheres Program. We also thank the anonymous referee for her/his helpful comments, and Jeremy King for several insightful discussions.

Facilities: Subaru

REFERENCES

- Allende Prieto, C., Lambert, D. L., & Asplund, M. 2001, *ApJ*, 556, L63
- Ammler-von Eiff, M., Santos, N. C., Sousa S. G., Fernandes, J., Guillot, T., Israelian, G., Mayor, M., Melo, C., 2009, *A&A*, 507, 523
- Asplund, M., Grevesse, N., Sauval, A. J., & Scott, P. 2009, *ARA&A*, 47, 481
- Bensby, T., Feltzing, S., & Lundström, I. 2004, *A&A*, 415, 155
- Bergfors, C., Brandner, W., Daemgen, S., et al. 2013, *MNRAS*, 428, 182
- Bergin, E. A. 2011, *Physical Processes in Circumstellar Disks around Young Stars*, 55
- Bond, J. C., O’Brien, D. P., & Lauretta, D. S. 2010, *ApJ*, 715, 1050
- Bubar, E. J., & King, J. R. 2010, *AJ*, 140, 293
- Buchhave, L. A., et al., 2012, *Nature*, 486, 375
- Burke, C. J., et al., 2007, *ApJ*, 671, 2115
- Caffau, E., Ludwig, H.-G., Steffen, M., Freytag, B., & Bonifacio, P. 2011, *Sol. Phys.*, 268, 255
- Cassan, A., et al. 2012, *Nature*, 481, 167
- Chambers, J. E. 2010, *ApJ*, 724, 92
- Crossfield, I. J. M., Barman, T., Hansen, B. M. S., Tanaka, I., & Kodama, T. 2012, *ApJ*, 760, 140
- Crouzet, N., McCullough, P. R., Burke, C., & Long, D. 2012, *ApJ*, 761, 7
- Cunha, K., Smith, V. V., & Lambert, D. L. 1998, *ApJ*, 493, 195

- Delgado Mena, E., Israelian, G., González Hernández, J. I., Bond, J. C., Santos, N. C.,
Udry, S., Mayor, M., 2010, *ApJ*, 725, 2349
- Désert, J.-M., Lecavelier des Etangs, A., Hébrard, G., Sing, D. K., Ehrenreich, D., Ferlet,
R., Vidal-Madjar, A., 2009, *ApJ*, 699, 478
- Fischer, D. A., & Valenti, J. 2005, *ApJ*, 622, 1102
- Fitzpatrick, M. J., & Sneden, C. 1987, *BAAS*, 19, 1129
- Fortney, J. J. 2012, *ApJ*, 747, L27
- Ghezzi, L., Cunha, K., Smith, V. V., de Araújo, F. X., Schuler, S. C., de la Reza, R., 2010,
ApJ, 720, 1290
- Gonzalez, G. 1998, *A&A*, 334, 221
- González Hernández, J. I., Israelian, G., Santos, N. C., Sousa, S., Delgado-Mena, E., Neves,
V., Udry, S., 2010, *ApJ*, 720, 1592
- Ida, S., & Lin, D. N. C. 2004, *ApJ*, 616, 567
- Kopparapu, R. k., Kasting, J. F., & Zahnle, K. J. 2012, *ApJ*, 745, 77
- Kuchner, M. J., & Seager, S. 2005, *arXiv:astro-ph/0504214*
- Kupka, F., Piskunov, N., Ryabchikova, T. A., Stempels, H. C., & Weiss, W. W. 1999,
A&AS, 138, 119
- Machalek, P., McCullough, P. R., Burrows, A., Burke, C. J., Hora, J. L., Johns-Krull,
C. M., 2009, *ApJ*, 701, 514
- Madhusudhan, N. 2012, *ApJ*, 758, 36
- Madhusudhan, N., et al. 2011, *Nature*, 469, 64

- Meléndez, J., Asplund, M., Gustafsson, B., & Yong, D. 2009, *ApJ*, 704, L66
- Narita, N., Hirano, T., Sato, B., Harakawa, H., Fukui, A., Aoki, W., Tamura, M., 2011, *PASJ*, 63, L67
- Nissen, P. E. 2013, *arXiv:1303.1726*
- Noguchi, K., et al. 2002, *PASJ*, 54, 855
- Öberg, K. I., Murray-Clay, R., & Bergin, E. A. 2011, *ApJ*, 743, L16
- Petigura, E. A., & Marcy, G. W. 2011, *ApJ*, 735, 41
- Ramírez, I., Meléndez, J., & Asplund, M. 2009, *A&A*, 508, L17
- Santos, N. C., Israelian, G., & Mayor, M. 2004, *A&A*, 415, 1153
- Schuler, S. C., Flateau, D., Cunha, K., King, J. R., Ghezzi, L., Smith, V. V., 2011a, *ApJ*, 732, 55
- Schuler, S. C., Cunha, K., Smith, V. V., Ghezzi, L., King, J. R., Deliyannis, C. P., Boesgaard, A. M., 2011b, *ApJ*, 737, L32
- Snedden, C. 1973, *ApJ*, 184, 839
- Stevenson, D. J., & Lunine, J. I. 1988, *Icarus*, 75, 146
- Swain, M. R., Vasisht, G., & Tinetti, G. 2008, *Nature*, 452, 329
- Takeda, Y. 2003, *A&A*, 402, 343
- Takeda, Y., & Honda, S. 2005, *PASJ*, 57, 65
- Tinetti, G., et al. 2007, *Nature*, 448, 169

Torres, G., Fischer, D. A., Sozzetti, A., Buchhave, L. A., Winn, J. N., Holman, M. J.,
Carter, J. A., 2012, ApJ, 757, 161

Valenti, J. A., & Piskunov, N. 1996, A&AS, 118, 595

Table 1. Lines Measured, Equivalent Widths, and Abundances

Ion	λ	χ	$\log gf$	EW_{\odot}	$\log N_{\odot}$	XO-2S		XO-2N	
						EW (mÅ)	$\log N$	EW (Å)	$\log N$
C I	5052.17	7.68	-1.304	27.1	8.31	36.4	8.61	33.0	8.77
	5380.34	7.68	-1.615	18.6	8.41	22.4	8.62	20.5	8.79
O I	6300.30	0.00	-9.717	5.4	8.63	10.7	8.81	11.5	8.97

Note. — This table is available in its entirety in a machine-readable form in the online journal. A portion is shown here for guidance regarding its form and content.

Table 2. Derived Stellar Parameters

Parameter ^a	XO-2S		XO-2N			
	this work	Burke et al. 2007	this work	Burke et al. 2007	Ammeler-von Eiff et al. 2009	Torres et al. 2012
T_{eff} (K)	5547±59	5500±32	5343±78	5340±32	5350±72	5450±75
$\log g$ (cgs)	4.22 ±0.24	4.62±0.05	4.49±0.25	4.48±0.05	4.14 ±0.22	4.45 ±0.02
ξ (km s ⁻¹)	1.24±0.07	...	1.22±0.09	...	1.10±0.08	...
[Fe/H]	0.28±0.14	0.47±0.02	0.39±0.14	0.45±0.02	0.42 ±0.07	0.27±0.11
[C/H]	0.26±0.11	...	0.42±0.12
[Ni/H]	0.38±0.04	0.52±0.02	0.44±0.04	0.50±0.02
[O/H]	0.18±0.15	...	0.34±0.16
C/O	0.60±0.19	...	0.60±0.20

^aAdopted solar parameters: $T_{\text{eff}} = 5777$ K, $\log g = 4.44$, and $\xi = 1.38$ km s⁻¹.

Note. — In this table the data listed as Torres et al. 2012 is only that derived from their MOOG-style analysis.

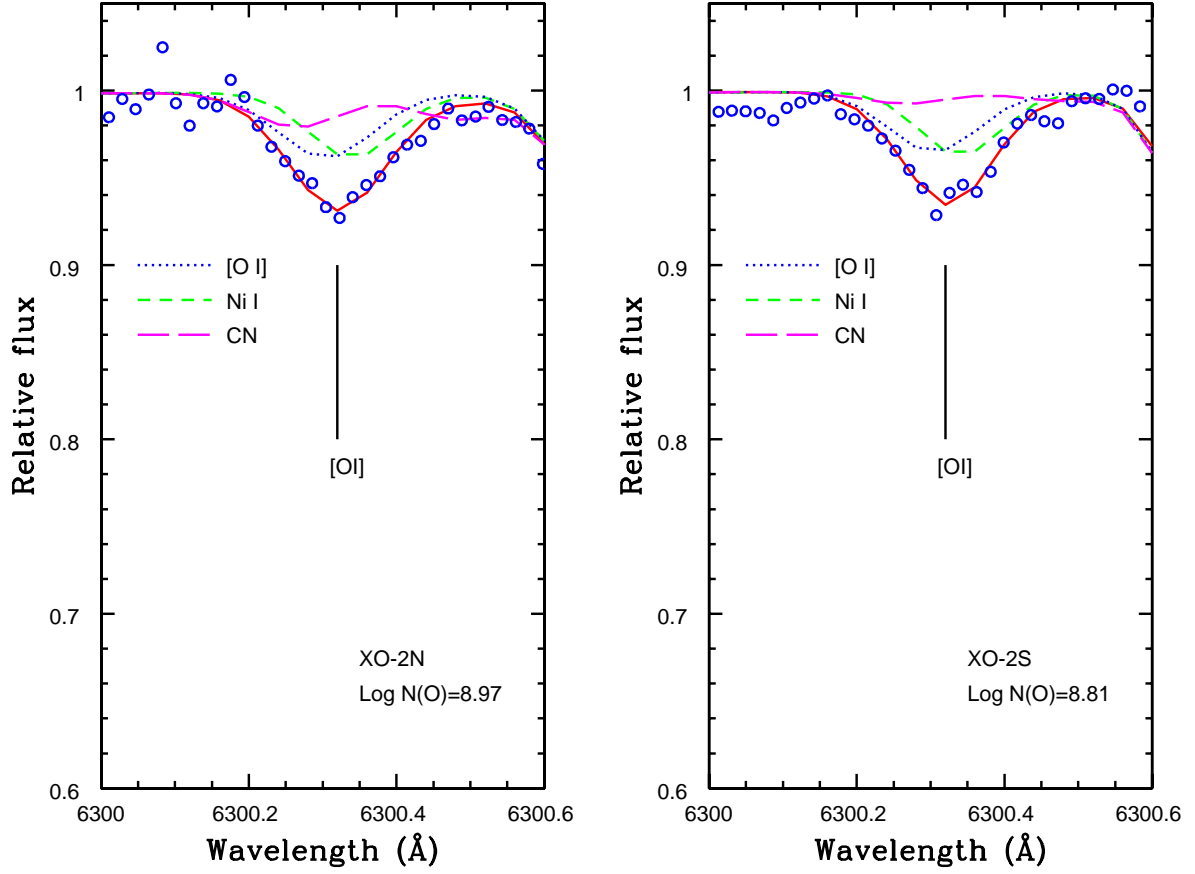


Fig. 1.— Shown are the spectrum synthesis fits to the forbidden [OI] line (6300.3 Å) for XO-2N (left) and XO-2S (right). The data are shown as blue open circles. The full synthesis fit is shown with a solid red line, with components shown with blue dotted ([OI]), green short-dashed (Ni I), and magenta long-dashed (CN) lines. Recall $\log(N_X)=\log_{10}(N_X/N_H)+12$.

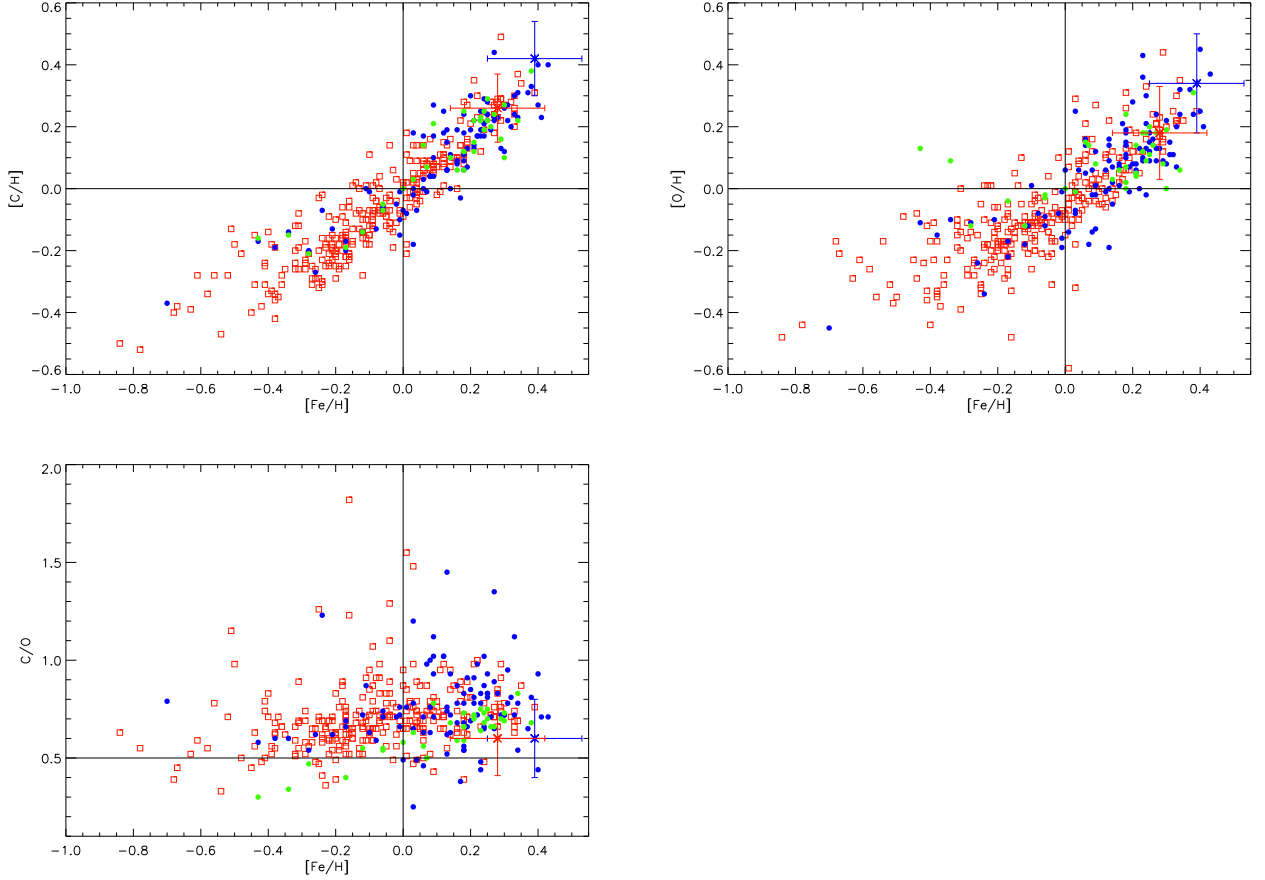


Fig. 2.— $[C/H]$, $[O/H]$, and C/O versus $[Fe/H]$ from Delgado Mena et al. (2010) and Nissen (2013) [all Nissen (2013) hosts are in the Delgado Mena et al. (2010) host sample]. Non-host stars from Delgado Mena et al. (2010) are plotted with red open squares, while host stars from Delgado Mena et al. (2010)/Nissen (2013) are plotted with blue/green circles. Measurements of XO-2N (blue) and XO-2S (red) from this work are plotted as asterisks, with error bars included (see Table 2). Black solid lines show the solar values.